Appl. Phys. B 68, 537–543 (1999)

**Applied Physics B**
Lasers
and Optics


# Role of optical interference effects in the enhancement of magnetization-induced second-harmonic generation

**T.V. Murzina*, A.A. Fedyanin, T.V. Misuryaev, G.B. Khomutov, O.A. Aktsipetrov****

Department of Physics, Moscow State University, 119899 Moscow, Russia

Received: 14 October 1998

**Abstract.** The role of optical interference in magnetization-induced effects in second-harmonic generation (SHG) is studied for magnetic nanostructures. The degree of magnetization-induced effects is governed by the fine-structure parameter and is subsequently small in low-order susceptibilities, yet enhanced at higher orders. One of the mechanisms of the enhancement of magnetization-induced contributions to the SHG intensity is related to the optical interference in the far-field region of the second-harmonic fields generated by nonmagnetic and magnetization-induced nonlinear polarizations. The model of interference is considered for resonant and off-resonant conditions in non-centro-symmetric media. This model is used for interpretation of experimental results of magnetization-induced SHG studies of Co nanocrystals and Gd monolayers.

**PACS:** 75.70.Ak; 75.70.Cn; 42.65

The role optical interference plays in nonlinear-optical phenomena is well known. As an example, the optical interference between the spectral background and resonant contribution to the third-order nonlinear susceptibility brings about a spectral shift of resonance wavelengths which is observed in coherent anti-Stokes Raman spectroscopy (CARS) [1]. The optical interference between contributions from first-order and quadratic susceptibilities stresses the appearance of weak absorption bands in spontaneous down-conversion spectroscopy [2]. The latter is an example how optical interference can serve as an amplifier for weak nonlinear-optical effects. Such an enhancement mechanism of (intrinsically) weak magnetization-induced effects in optical second-harmonic generation (SHG) has recently received significant attention [3].

Magnetization-induced SHG (MSHG) is a sensitive probe of surfaces and interfaces of magnetized media and magnetic thin films [4]. The surface sensitivity of MSHG arises from the general sensitivity of SHG to the breakdown of symmetry. Different types of symmetry breakdown can play a role in the unique sensitivity of SHG to the structural, electronic and magnetic properties of surfaces, interfaces and nanostructures [4–6]. For example, the unusually high surface/interface sensitivity of the SHG probe of centrosymmetric materials comes about because, in the electric dipole approximation, SHG is forbidden in the bulk of materials with inversion symmetry [5], but allowed at interfaces, where inversion symmetry is broken by the discontinuity of crystalline structure.

Another domain of the nonlinear optics of low-dimensional systems appears as the breakdown of the structural inversion symmetry is combined with the broken time reversal symmetry due to the magnetization of a magnetic material.

There are two distinct differences between magnetization-induced and electro- induced nonlinear-optical responses. First, in contrast to a DC electric field, a DC magnetic field, being an axial vector, does not break inversion symmetry in centro-symmetric materials. A magnetic field breaks time reversal symmetry instead. Second, since magnetization-induced effects follow that of the fine-structure parameter, they are intrinsically much smaller then electro-induced phenomena. The former demands that the material structure has no inversion symmetry for the appearance of dipole magnetization-induced susceptibilities. The latter demands extremely large internal magnetic fields in magnetized material or the existence of mechanisms that enhance magnetization-induced changes in nonlinear-optical responses.

MSHG has been one of the most intensively studied phenomena in surface and interface nonlinear optics for the last decade. The interest in the MSHG effects can be traced back to the theoretical paper by Zvezdin and co-workers, published in 1985, where the bulk MSHG was predicted [7]. The theoretical description of the MSHG surface sensitivity was first carried out by Shen and co-workers [8], where they showed that the magnetization could change the symmetry and the structure of the tensor of the surface nonlinear susceptibility. The detailed calculations of the surface magnetic second-order susceptibility were made by Hübner, Bennemann and Pustogowa [9–12].

* E-mail: mur@astral.ilc.msu.su
** E-mail: aktsip@astral.ilc.msu.su; Web: http://kali.ilc.msu.su

Since the experimental observations of the 1988s, MSHG has been intensively studied in a variety of systems. First, the nonlinear magneto-optical Kerr effect (NOMOKE)[1] and the nonlinear-optical Faraday effect (NFE) were observed in thin iron garnet films [13] and $Cr_2O_3$ single crystals [14]. Then Kirschner and co-workers [15] and Matthias and co-workers [16] observed NOMOKE from clean Fe(110) and MnPtSb(111) surfaces under UHV conditions. The relation between the interface magnetism and SHG in multilayered magnetic structures has been intensively studied by Rasing and co-workers [17–20]. Recently, interest in the MSHG effects in garnet films was rejuvenated by Pisarev, Fröhlich and co-workers [21–23].

In this paper, the role of an interference in the enhancement of the magnetization-induced effects in SHG is considered for the case of magnetic low-dimensional structures. The experimental studies of MSHG are carried out for Co-Cu granular films and Gd-containing Langmuir–Blodgett (LB) films. The interference between nonmagnetic and magnetization-induced components of second-harmonic (SH) fields is considered as an "amplifier" for the magnetization-induced changes in SH response for these structures.

## 1 Enhancement of MSHG effects due to optical interference (non-centro-symmetric magnetic medium)

In the following, a simple phenomenological model of MSHG effects, which takes into account an interference of SH fields, is considered for a qualitative interpretation of experimental results. The SHG intensity in the far-field region from a semi-infinite medium is given by

$$I_{2\omega} \propto \left|\boldsymbol{E}^{\mathrm{S}}(2\omega) + \boldsymbol{E}^{\mathrm{B}}(2\omega)\right|^2 , \tag{1}$$

where $\boldsymbol{E}^{\mathrm{S}}(2\omega)$ and $\boldsymbol{E}^{\mathrm{B}}(2\omega)$ are the SH fields generated by surface and bulk nonlinear polarizations, respectively. In a gyrotropic medium they contain nonmagnetic (crystallographic) and magnetization-induced components. In the following, only components of the quadratic susceptibility $\chi^{(2)}$ that possess odd parity with respect to magnetization $\boldsymbol{M}$, i.e. that change their sign under the inversion of $\boldsymbol{M}$, will be considered: $\chi^{(2)\mathrm{M}}_{ijkl}(M) = -\chi^{(2)\mathrm{M}}_{ijkl}(-M)$. The $i$-th component of the SH field generated by the surface, $\boldsymbol{E}^{\mathrm{S}}(2\omega)$, is given by

$$\begin{aligned} E^{\mathrm{S}}_i(2\omega) &\propto \int\limits_{\Delta z} \left(P^{\mathrm{SCr}}_i(2\omega) + P^{\mathrm{SM}}_i(2\omega, M)\right) G_0 \,\mathrm{d}z' \\ &\propto \chi^{(2)\mathrm{Sd}}_{ijk} E^{\omega}_j E^{\omega}_k + \mathrm{e}^{\mathrm{i}\varphi_1} \chi^{(2)\mathrm{SdM}}_{ijkl} E^{\omega}_j E^{\omega}_k M_l , \end{aligned} \tag{2}$$

where $P^{\mathrm{SCr}}_i(2\omega)$ and $P^{\mathrm{SM}}_i(2\omega, M)$ are the $i$th components of the surface nonmagnetic and magnetization-induced nonlinear polarizations, respectively; $\chi^{(2)\mathrm{Sd}}_{ijk}$ and $\chi^{(2)\mathrm{SdM}}_{ijkl}$ are the dipole surface, nonmagnetic and magnetic susceptibilities, respectively, and $\varphi_1$ is the phase shift between them; $E^{\omega}_j$ is the component of the fundamental field; $G_0$ is the Green function for the surface nonlinear sources; the integration is over the subsurface layer $\Delta z$. It is important that $G_0$ gives only a numerical factor, $g_0$, in the nonlinear polarization and does not change the phase of the SH fields generated by the surface polarizations. In a transparent magnetic material away from resonance $\varphi_1 = \pi/2$. The bulk $i$-th component of the SH field is given by:

$$\begin{aligned} E^{\mathrm{B}}_i(2\omega) &= \int\limits_0^{\infty} G_{ij}(z, z') P^{\mathrm{B}}_j(z', 2\omega) \,\mathrm{d}z' \\ &\propto \frac{i}{\Delta k} A_{ij} \left(\chi^{(2)\mathrm{Bd}}_{jkl} E^{\omega}_k(z) E^{\omega}_l(z) + \mathrm{e}^{\mathrm{i}\varphi_2} \chi^{(2)\mathrm{BdM}}_{jklm} \right. \\ &\quad \left. \times E^{\omega}_k(z) E^{\omega}_l(z) M_m\right) , \end{aligned} \tag{3}$$

where $P^{\mathrm{B}}(z', 2\omega)$ is the bulk nonlinear polarization; $G(z, z')$ is the Green function of the nonlinear wave equation for the bulk nonlinear polarization; $\chi^{(2)\mathrm{Bd}}_{jkl}$ and $\chi^{(2)\mathrm{BdM}}_{jklm}$ are the dipole bulk nonmagnetic and magnetic susceptibilities (which are real quantities in a transparent media), respectively, and $\varphi_2$ is the phase shift between them; $\Delta k = 2k_{\omega} - k_{2\omega}$ is the phase mismatch; $k_{\omega}$ and $k_{2\omega}$ are the fundamental and SH wave vectors, respectively. For the reflection configuration of the MSHG experiment (NOMOKE) the phase mismatch $|\Delta k| \approx |k_{\omega}|$, and in transmission (NFE) $|\Delta k| \ll |k_{\omega}|$. For a transparent film, the $A_{ij}$ are real constants.

Thus the MSHG intensity, (1), takes the form

$$\begin{aligned} I_{2\omega} \propto |\boldsymbol{E}(2\omega)|^2 &= \left|\boldsymbol{E}^{\mathrm{Sd}}(2\omega) + i\boldsymbol{E}^{\mathrm{SdM}}(2\omega, M) + i\hat{K}\left(\boldsymbol{E}^{\mathrm{Bd}}(2\omega) \right.\right. \\ &\quad \left.\left. + i\boldsymbol{E}^{\mathrm{BdM}}(2\omega, M)\right)\right|^2 \\ &\propto \left|\left(\chi^{(2)\mathrm{Sd}}_{ijk} + i\chi^{(2)\mathrm{SdM}}_{ijkl} M_l + iK_{ij}\chi^{(2)\mathrm{Bd}}_{jkl} \right.\right. \\ &\quad \left.\left. - K_{ij}\chi^{(2)\mathrm{BdM}}_{jklm} M_m\right) E^{\omega}_j E^{\omega}_k\right|^2 , \end{aligned} \tag{4}$$

where $K_{ij}$ are real constants for a transparent film.

It is readily seen from (4) that at off-resonance, as $\varphi_1 = \varphi_2 = \pi/2$, i.e. *odd* magnetization changes in the SHG intensity and phase are determined by the interference of the magnetization-induced SH fields and those independent from magnetization and are described by surface-bulk cross-terms like $\chi^{(2)\mathrm{Sd}}_{ijk}\,\chi^{(2)\mathrm{BdM}}_{jklm} M_m$ and $\chi^{(2)\mathrm{Bd}}_{jkl}\,\chi^{(2)\mathrm{SdM}}_{ijkl} M_l$.

Under pre-resonant or resonant conditions such as $\varphi_1 \neq \pi/2$ and $\varphi_2 \neq \pi/2$, a number of nonmagnetic/magnetization-induced cross-terms of the SH fields can appear in (4). In this case the SH fields from the non-centro-symmetric bulk of the film are supposed to be the main contribution to SHG intensity, and the largest contribution to odd magnetization changes of the SHG response are described by the term $\chi^{(2)\mathrm{Bd}}_{jkl}\,\chi^{(2)\mathrm{BdM}}_{ijkl} M_l$.

It is worth noting that MSHG effects have been considered in semi-infinite magnetic media. For films of finite thickness or for particles of finite size, the tensor elements $A_{ij}$ and $K_{ij}$ in (3) and (4) should be complex. This will bring about the appearance of additional cross-terms in (4), both at a resonant and off-resonant fundamental wavelength.

[1] The description of NOMOKE introduced in recent papers is somewhat misleading since it could be related to the nonlinear dependence of an angle of the linear magneto-optical Kerr rotation on the magnitude of a DC magnetic field.

## 2 Experimental set-up

In MSHG studies the output of a Q-switched YAG:$Nd^{3+}$ laser at 1064 nm is used as a fundamental radiation with a pulse duration of 15 ns, a repetition rate of 12.5 Hz, and a pulse intensity of about 1 MW/cm$^2$. The SHG radiation reflected from the samples at an angle of 45° is filtered out from the spectral background by a double monochromator or band-pass filters, and detected by a PMT and gated electronics.

For the characterization of nonlinear magneto-optical properties of low-dimensional magnetic structures we measure SHG anisotropy (dependence of the SHG intensity on an azimuthal angle) and the magnetization-induced phase shift of the SH wave (MSHG interferometry), and polarization diagrams (dependence of the MSHG intensity on an analyzer angle) for two opposite directions of a DC-magnetic field. The MSHG interferometry [24] is performed in the conventional "single-beam" scheme. In this method, the SHG signal of interfering SH waves from the reference and the sample is measured as a function of the position $d$ of the reference for the two opposite directions of the DC-magnetic field. A 50-nm-thick $SnO_2$ film serves as a source of the coherent SH response (reference). The coherence of the SHG response from the sample is characterized by the mutual coherence $\alpha$ of the interfering SH waves ($0 < \alpha < 1$).

## 3 MSHG studies of Co-Cu granular films

### *3.1 Sample preparation and characterization*

Magnetic $Co_xCu_{1-x}$ granular films of about 200 nm thickness were prepared by the co-deposition of Co and Cu in a dual electron-beam evaporator at the residual pressure of $10^{-4}$ Pa on a glass substrates. The deposition rate of Co was kept constant at 0.05 nm/s, while the deposition rate of Cu was varied from 0.05 to 2 nm/s to produce films of various compositions. The $Co_xCu_{1-x}$ films ($x = 0.09$, 0.19, 0.42, 0.51, 0.56) were annealed at 400 K for 30 min.

The structure of the films was characterized by X-ray diffraction, electron diffraction and scanning tunneling microscopy (STM). The X-ray diffraction patterns show that the $Co_xCu_{1-x}$ films consist of a metastable solid solution with *fcc* crystalline structure. The diffraction patterns show that the mean crystallite size of Co granules ranges from 80 nm to 40 nm as the Co concentration varies from 0.09 to 0.56. The STM measurements carried out in air reveal irregular shap distortion from the spheroidal form for the topmost granules at the film–air interface.

### *3.2 Azimuthal SHG anisotropy and* Co *concentration dependence of SHG from* $Co_xCu_{1-x}$ *granular films*

The structure of the surface layer of the $Co_xCu_{1-x}$ granular films was studied by measuring the azimuthal anisotropy of the SHG intensity. Figure 1 shows such dependences for three polarization combinations of the fundamental and SH waves. The sufficient two-fold and four-fold symmetry of the SHG anisotropy is found for the $s$-in/$s$-out and $p$-in/$s$-out polarization combinations, respectively. The four-fold symmetry of the SHG anisotropy combined with a strong one-fold

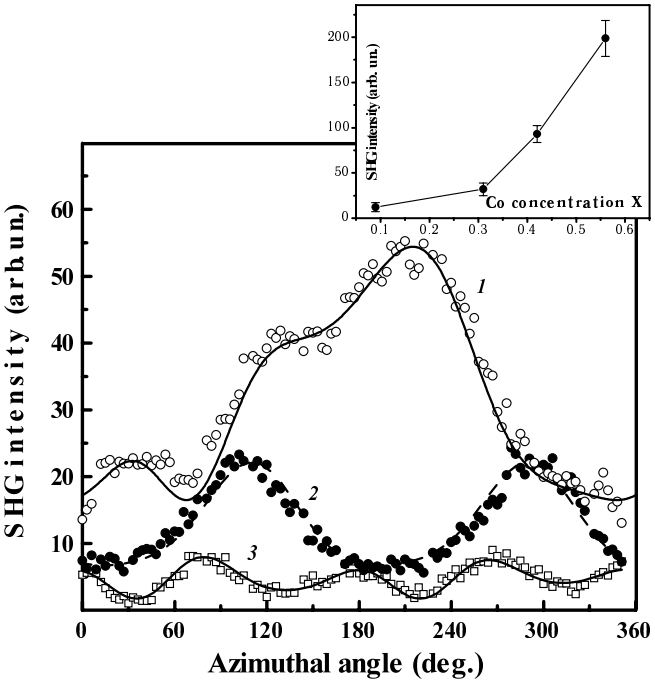


**Fig. 1.** The azimuthal angular dependencies of the SHG intensity for $Co_{0.42}Cu_{0.58}$ granular magnetic films for $p$-in/$p$-out (1), $s$-in/$s$-out (2) and $p$-in/$s$-out (3) polarization combinations. Inset: dependence of the $p$-$p$ SHG intensity maximum on the relative Co concentration in $Co_xCu_{1-x}$ granular films

pattern is observed for $p$-in/$p$-out polarization combination. Such SHG anisotropy can be attributed to the existence of a polar axis in the symmetry elements of the film structure, tilted with respect to the normal to the film surface. The origin of such a structure can be a regular deviation of the particle shape from centrosymmetric. As a consequence, the appearance of the polar axis in the topmost array of Co nanocrystals can be caused by a predominant regular asymmetry of the film–vacuum interface due to the co-deposition during the film processing. This should lead to the appearance of a coherent (regular) dipole-type contribution to the nonlinear polarization from the topmost layer of the array of non-centro-symmetric Co granules.

The inset in Fig. 1 shows the $x$ dependence of the maximum of the $p$-in/$p$-out SHG intensity. The SHG signal from the Co-free Cu film is much smaller than the signal from the $Co_{0.09}Cu_{0.91}$ film. The Co concentration dependence of the SHG intensity, which is close to quadratic, indicates a regular contribution from the array of Co nanocrystals probed by SHG. Otherwise, this dependence is expected to be linear as in the case of incoherent SHG (hyper-Rayleigh scattering).

### *3.3 NOMOKE in* Co-Cu *granular films*

Polar, transverse and longitudinal NOMOKE is studied and compared with the results of spectroscopic measurements of magnetic optical Kerr effect (MOKE). For the transversal magnetization MOKE is characterized by the magnetic contrast, $\rho_\omega = (I_\omega(M^+) - I_\omega(M^-))/((I_\omega(M^+) + I_\omega(M^-))$, where $I_\omega(M^+)$ and $I_\omega(M^-)$ are the intensities of the reflected light for the two opposing directions of the magnetization.

The AC magnetic field amplitude in the MOKE measurements was 3.0 kOe at a frequency of 80 Hz. Transverse MOKE for the $Co_xCu_{1-x}$ films was measured in the energy range of 1.2–3.6 eV. The inset in Fig. 2 shows the concentration dependence of the MOKE magnetic contrast at 1.17 eV and 2.34 eV.

In the NOMOKE studies, a DC magnetic field up to 1 kOe is applied. The magnetization-induced changes in the SHG intensity, which possess odd parity with respect to magnetization, are characterized by magnetic contrast, $\rho_{2\omega} = [I_{2\omega}(M^+) - I_{2\omega}(M^-)]/[I_{2\omega}(M^+) + I_{2\omega}(M^-)]$, where $I_{2\omega}(M^+)$ and $I_{2\omega}(M^-)$ are the SHG intensities for the two opposing directions of magnetization. The magnetic contrast of transverse NOMOKE is measured for $Co_{0.42}Cu_{0.58}$ granular films at a 50° angle of incidence and is found to be approximately $4 \times 10^{-2}$. The analogous MOKE contrast measured at the wavelengths 532 nm and 1064 nm is approximately $10^{-3}$. Therefore, the magnitude of transverse NOMOKE is about 40 times larger than that of the transverse MOKE. Similar NOMOKE enhancement, with respect to MOKE, is obtained for the films of various compositions.

Figure 2 shows the polarization SHG diagrams, i.e. the dependences of the SHG intensity on the angular position of the analyzer, for polar NOMOKE in a $Co_{0.42}Cu_{0.58}$ film. The angle of Kerr rotation of the SH wave polarization is approximately 7°, whereas for polar MOKE, the corresponding rotation angles at the fundamental and SH wavelengths appear to be at least an order of magnitude smaller. Thus, both polar and transverse NOMOKE exceed the linear analogues by more than an order of magnitude.

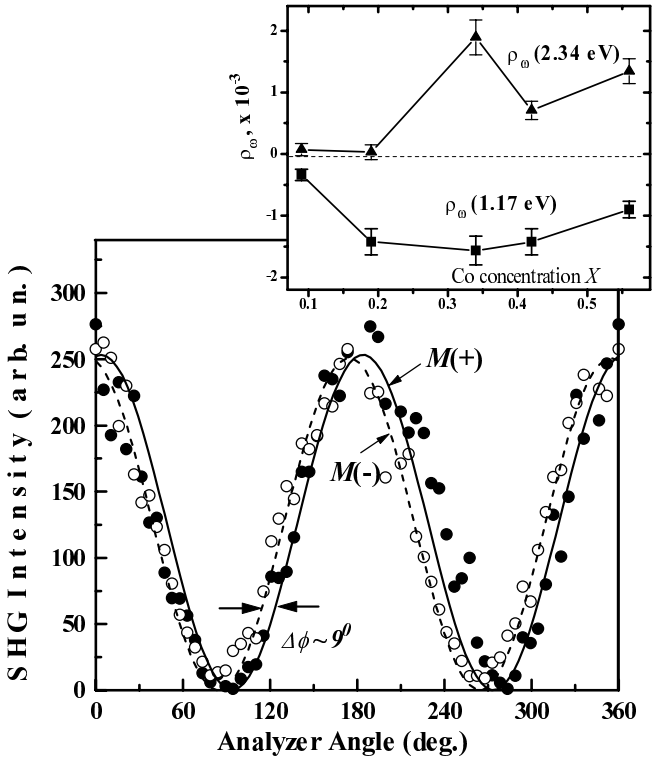


**Fig. 2.** The dependence of the MSHG intensity on the analyzer angle (MSHG polarization diagram) for polar NOMOKE of the $Co_{0.42}Cu_{0.58}$ film for the two directions of magnetization. Inset: Co concentration dependence of the MOKE magnetic contrast at the fundamental and SH wavelengths

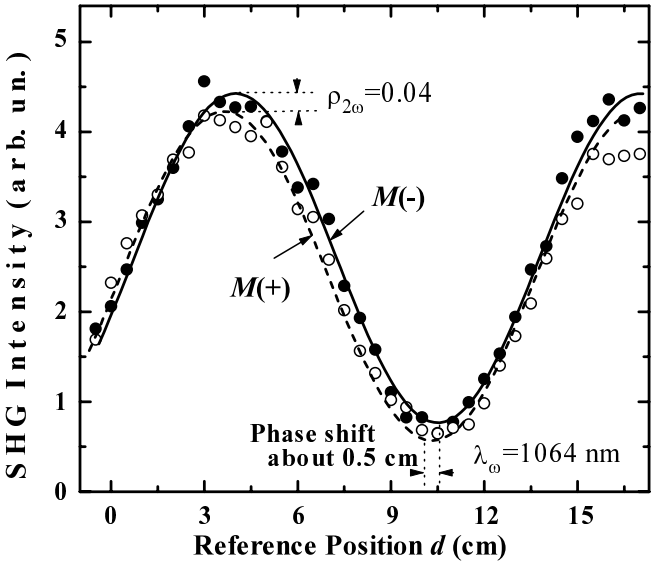


**Fig. 3.** The dependence of MSHG intensity on the reference position (MSHG interference pattern) for the transverse NOMOKE in the $Co_{0.42}Cu_{0.58}$ film for the two directions of magnetization

The magnetization-induced phase shift of the SH wave in the Co-Cu granular films is measured for the transverse NOMOKE. Figure 3 shows the dependence of the MSHG intensity on the reference position for a $Co_{0.42}Cu_{0.58}$ film. It can be seen that the factor of mutual coherence of interfering SH waves from the sample and the reference $\alpha$ is close to unity, which indicates, first, that the SH wave generated by the array of the Co nanocrystals is sufficiently coherent (regular), and, second, that there is mutual coherence between the nonmagnetic and magnetic contributions to the total SH field. The magnetization-induced shift of the interference patterns in Fig. 3 is approximately 0.5 cm, which corresponds to approximately 8° in the phase domain.

### *3.4 Interference mechanism of NOMOKE in* Co-Cu *granular films*

In accordance with the phenomenological model described in Sect. 1, large changes in the SHG intensity that possess odd parity with respect to magnetization can be expected because of the interference between the dipole-like nonmagnetic and (intrinsically small) magnetization-induced SH fields. This requires the simultaneous break-down of the structural inversion symmetry of the sample and the time-reversal symmetry.

First, break-down of the time-reversal symmetry in Co nanocrystals takes place as a result of the magnetization. Second, at least two mechanisms can be responsible for the appearance of the dipole susceptibility $\chi^{(2)d}$ in metal nanocrystals. The first one is the surface dipole $\chi^{(2)Sd}$, which stems from the lack of inversion symmetry at the surfaces and interfaces of centrosymmetric media [5]. The second mechanism of the bulk dipole $\chi^{(2)Bd}$ in metallic nanocrystals is related to the breaking of inversion symmetry in particles with noncentro-symmetric geometrical shape [25]. The deviation of the particle shape from a centro-symmetric (spheroidal) shape violates the rule forbidding the dipole $\chi^{(2)Bd}$ in nanocrystals of centro-symmetric materials. Both these mechanisms give

rise to a dipole quadratic susceptibility of Co nanocrystals in granular films. The mutual coherence of the nonlinear contributions from the nonmagnetic and magnetic sub-systems of the metallic Co nanocrystals obtained by the MSHG interferometry also indicates the existence of the regular $\chi^{(2)B}$ in $Co_xCu_{1-x}$ granular films. In principle, one can expect incoherent SHG (hyper-Rayleigh scattering) from an array of Co nanocrystals with shape distortion. However, the MSHG interference patterns show the regular (coherent) magnetic SH contribution. This magnetic contribution, attributed to the external magnetic field, is coherent with the nonmagnetic nonlinear polarization.

Thus, the model of MSHG described in Sect. 1 can be applied to Co-Cu granular films because of a simultaneous break-down of inversion and time-reversal symmetry in Co nanocrystals. The interference cross-terms can be significant in the MSHG intensity from Co-Cu granular films because of the appearance of $\chi^{(2)Sd}$ and $\chi^{(2)Bd}$ in metallic nanocrystals and because of resonant conditions in metallic Co particles of finite size.

## 4 MSHG in magnetic Gd-containing Langmuir–Blodgett films

### *4.1 Film preparation and characterization*

The LB films are deposited on fused quartz substrates by the Langmuir–Blodgett technique. Figure 4a shows a schematic view of LB films deposition. A solution of stearic acid in chloroform spread on the water surface is used. The Gd acetate of the concentration $5 \times 10^{-4}$ M is dissolved in water, which results in the adsorption of $Gd^{3+}$ ions from the water solution on the solid stearic acid Langmuir monolayer. This method gives the Gd-containing LB films with a structural unit (SU) composed by the monolayer of Gd ions situated between two monolayers of stearic acid molecules (Fig. 4a). Films composed of 40 structural units are studied. The area per Gd ion in the monolayer is approximately 10 Å$^2$.

Figure 4b shows the glancing-angle X-ray diffraction pattern obtained for Gd-containing LB films with 10 structural units from the same set of the samples. This diffraction pattern demonstrates a well-defined layered periodic structure of Gd ions with the period of approximately 50 Å. The angular width of the diffraction peaks ($\approx 0.1°$) yields a coherence length of the order of hundreds of nanometers.

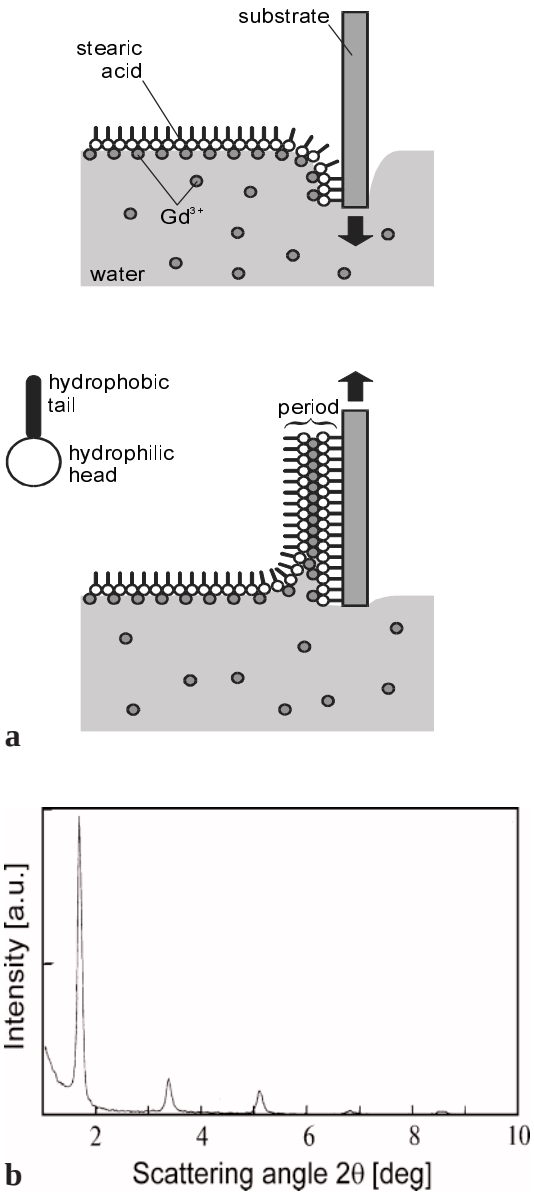


**Fig. 4a,b.** Schematic of the LB technique with vertical lift and the composition of the structural unit of the Gd-containing LB films (**a**); X-ray diffraction pattern for Gd-containing LB film consisting of 10 structural units (**b**)

### *4.2 General properties of SHG radiation in* Gd*-containing LB films*

SHG from Gd-containing LB films is attributed to the presence of gadolinium ions and/or gadolinium-stearic acid organo-metallic complexes in the LB film structural unit. This stems from the fact that the SHG intensity from both the quartz substrate and LB films of Gd-free stearic acid is found to be negligibly small. The SHG radiation is shown to be strongly diffuse, i.e. apart from the SHG response in the specular direction, a significant part of the SHG signal is scattered in the nonspecular direction. No distinct anisotropy of the SHG response is observed, whereas there is a sufficient *s*-polarized SHG response which is forbidden for a homogeneous isotropic media. This is typical for incoherent SHG or, in other words, hyper-Rayleigh scattering (HRS).

### *4.3 NOMOKE studies in* Gd*-containing LB films*

Magnetization-induced effects in SHG from Gd-containing LB films are studied by MSHG interferometry and MSHG polarization diagrams. Figure 5 shows the SH polarization diagrams measured for the magnetic field of $\pm 1$ kOe and for the *s*-polarized fundamental radiation. The angle of the magnetization-induced rotation of the SH wave polarization is approximately 12°. In comparison with characteristic values of MOKE rotation for Gd single crystals, NOMOKE exceeds MOKE parameters by approximately two orders of magnitude.

Figure 6 shows the MSHG interferometry patterns measured for the longitudinal NOMOKE for the *s*-in/*s*-out and *p*-in/*p*-out polarization combinations. The SHG interferomet-

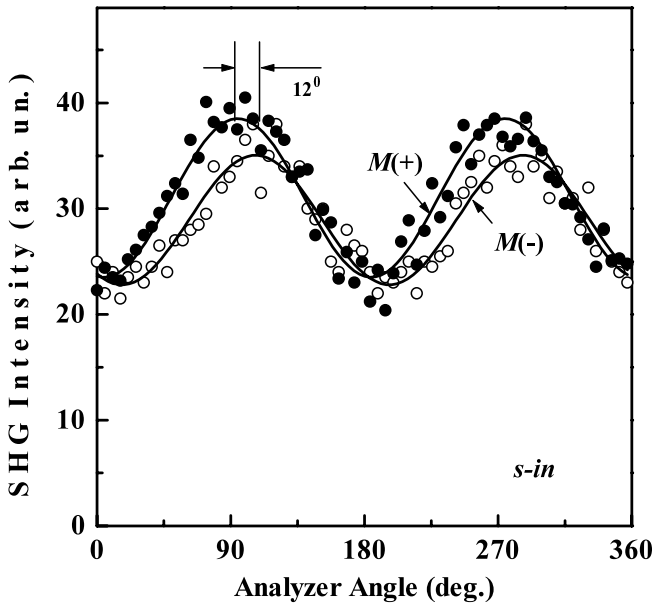


**Fig. 5.** The MSHG polarization diagrams for longitudinal NOMOKE in the Gd-containing LB film consisting of 40 structural units for opposite directions of magnetization

ric pattern for the *s*-in/*s*-out polarization combination shows the partial interference of the SH waves from the reference and the sample. The change of sign of an applied DC magnetic field leads to the shift of the interferometric pattern of approximately 115°. For the *p*-in/*p*-out polarization combination no changes in interference patterns are observed under the inversion of a DC magnetic field, while the partial coherence remains for the SH response from the LB films.

### *4.4 Interference mechanism of MSHG in Gd-containing LB films*

It is shown in Sect. 4.2 that SHG and MSHG responses from Gd-containing LB films is attributed to the presence of Gd ions and/or their aggregates. X-ray diffraction reveals a perfect multilayer periodic structure of LB films which indicates that Gd ions are combined in flat two-dimensional layers. At the same time, a diffuseness and depolarization of SHG indicates that the distribution of the nonlinear sources is inhomogeneous. This inhomogeneity can result from spatial fluctuations of the random distribution of Gd ions within LB structural units and should be attributed to an in-plane inhomogeneity of Gd monolayers. This in-plane inhomogeneity appears as the Gd ions are combined within a monolayer in 2D islands. Such a construction of a LB film should possess a dipole quadratic susceptibility to reveal magnetization-induced effects in SHG. By analogy with Co granules, shape-distortion mechanism of the dipole quadratic susceptibility can be supposed for these 2D Gd islands with non-centrosymmetric geometrical shape. At the same time, individual Gd ion in a structural unit of LB films (Fig. 4a) is supposed to be centro-symmetric and thus a noticeable dipole nonlinearity and, as a consequence, noticeable contribution to magnetization-induced effects is hardly expected. Thus, the electric-dipole susceptibility of such a structure can be caused

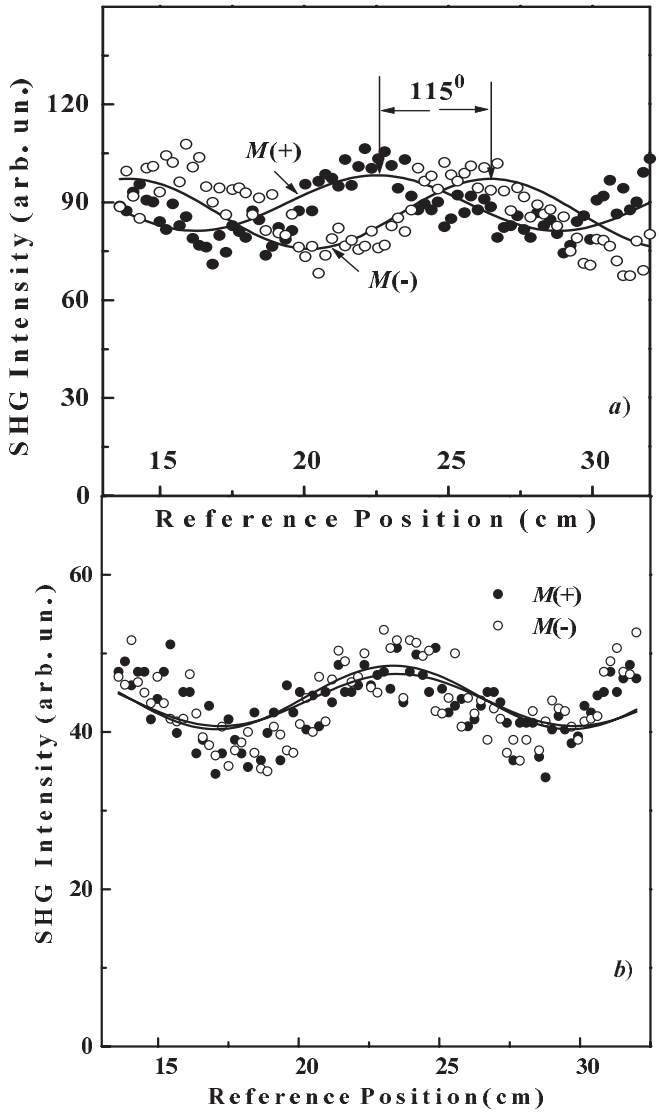


**Fig. 6a,b.** The MSHG interference patterns for the longitudinal NOMOKE in the Gd-containing LB films consisting of 40 structural units for opposite directions of magnetization: *s*-in/*s*-out polarization combination (**a**); *p*-in/*p*-out polarization combination (**b**)

by the presence of gadolinium 2D islands with an in-plane non-centro-symmetric geometrical shape.

The large angle of magnetization-induced rotation of the SH wave polarization and the large magnetization-induced variations of the SH wave phase indicate a strong coupling between nonlinear optical and magnetic properties of the film. In accordance with the model in Sect. 1, this can take place as the magnetic film possesses a *nonmagnetic* electric-dipole susceptibility. In this case, optical interference between *nonmagnetic* and *magnetization-induced* nonlinear polarizations leads to an enhancement of magnetization- induced effects in SHG.

## 5 Conclusions

The structural and magnetic properties of magnetic Co nanocrystals imbedded in the Cu matrix have been studied

by means of magnetization-induced SHG. The symmetry of the azimuthal SHG anisotropy and the MSHG interferometry shows the existence of the regular bulk dipole contribution to the quadratic polarization of individual Co granules. This dipole second-order susceptibility of metallic granules results from the non-centro-symmetric granule shape. A significant nonlinear magneto-optical Kerr effect is observed in SHG from Co-Cu granular films. The enhancement of magnetic effects is attributed to the cross-terms in the MSHG intensity stemming from optical interference in the far-field region of the nonmagnetic and magnetization-induced nonlinear contributions to the SH field.

The structural and magnetic properties of Langmuir–Blodgett films containing Gd monolayers are studied by means of MSHG. The combination of X-ray diffraction with nonlinear optical studies shows that, on the one hand, Gd-containing LB films possess a perfectly layered structure ordered in a direction normal to the film surface. On the other hand, the structural unit of LB films is composed by an inhomogeneous layer of Gd ions squeezed between two monolayers of stearic acid molecules. Within the single structural unit, Gd ions are assembled in 2D islands with random non-centro-symmetrical shape. A significant nonlinear magneto-optical Kerr effect, which manifests itself in magnetization-induced changes of the polarization and phase of the second-harmonic wave and SHG intensity, is observed. The mechanism of NOMOKE is interpreted in terms of optical interference between SH fields from the dipole nonlinear polarization of the electronic subsystem of non-centro-symmetric Gd islands and magnetization-induced nonlinear contribution of their spin subsystem.

*Acknowledgements.* This work was supported by INTAS-93-370(ext) and INTAS-YSF-8, 10 grants, Russian Foundation of Basic Research (RFBR) grants 97-02-17919 and 97-02-17923, Special RFBR grant for Russian Leading Scientific Schools 96-15-96420, Federal Integration Program “Center of Fundamental Optics and Spectroscopy” and Program of Russian Ministry of Science “Physics of Solid State Nanostructures”.

## References

1. N.I. Koroteev, M. Endemann, R.L. Byer: Phys. Rev. Lett. **43**, 398 (1979)
2. O.A. Aktsipetrov, G.M. Georgiev, I.V. Mityusheva, A.G. Mikhailovskii, A.N. Penin: Sov. Phys. Solid State **17**, 1324 (1975)
3. O.A. Aktsipetrov, A.A. Fedyanin, A.V. Melnikov, E.D. Mishina, T.V. Murzina: Jpn. J. Appl. Phys. **36**, 48 (1998)
4. Th. Rasing: J. Magn. Magn. Mater. **165**, 35 (1997)
5. T.F. Heinz: In *Nonlinear Surface Electromagnetic Phenomena*, ed. by H.-E. Ponath, G.I. Stegeman (North Holland, Amsterdam 1991) p. 355
6. O.A. Aktsipetrov, P.V. Elyutin, A.A. Fedyanin, A.A. Nikulin, A.N. Rubtsov: Surf. Sci. **325**, 343 (1995)
7. N.N. Akhmediev, S.B. Borisov, A.K. Zvezdin, I.L. Lyubchanskii, Yu.V. Melnikov: Sov. Phys. Solid State **27**(4), 650 (1985)
8. R.P. Pan, H.D. Wei, Y.R. Shen: Phys. Rev. B **39**, 1229 (1989)
9. U. Pustogowa, W. Hübner, K.H. Bennemann: Phys. Rev. B **48**, 8607 (1993)
10. U. Pustogowa, W. Hübner, K.H. Bennemann: Appl. Phys. A **59**, 611 (1994)
11. U. Pustogowa, W. Hübner, K.H. Bennemann, T.A. Luce: J. Appl. Phys. **79**, 6177 (1996)
12. U. Pustogowa, W. Hubner, K.H. Bennemann, T. Kraft: Z. Phys. B **102**, 109 (1997)
13. O.A. Aktsipetrov, O.V. Braginskii, D.A. Esikov: Proceedings of ICONO-13 (Minsk, USSR, 1988) v. 2, p. 142 (1988); Sov. J. Quant. Electron. **20**, 259 (1990)
14. A.M. Agal’tsov, V.S. Gorelik, A.K. Zvezdin, V.A. Murashov, D.N. Rakov: Sov. Phys. Lebedev Institute Reports **5**, 48 (1989)
15. J. Reif, J.C. Zink, C.M. Schneider, J. Kirschner: Phys. Rev. Lett. **67**, 2878 (1991)
16. J. Reif, C. Rau, E. Matthias: Phys. Rev. Lett. **71**, 1931 (1993)
17. G. Spierings, V. Koutsos, H.A. Wierenga, M.W.J. Prins, D. Abraham, Th. Rasing: J. Magn. Magn. Mater. **121**, 109 (1993)
18. B. Koopmans, M.G. Koerkamp, Th. Rasing, H. van den Berg: Phys. Rev. Lett. **74**, 3692 (1995)
19. Th. Rasing, M. Groot Koerkamp, B. Koopmans, H. van den Berg: J. Appl. Phys. **79**, 6181 (1996)
20. A. Kirilyuk, Th. Rasing, B. Doudin: J. Appl. Phys. **81**, 4723 (1997)
21. R.V. Pisarev, B.B. Krichevtsov, V.N. Gridnev, V.P. Klin, D. Fröhlich, Ch. Pahlke-Lerch: J. Phys. **5**, 8621 (1993)
22. V.V. Pavlov, R.V. Pisarev, A. Kirilyuk, Th. Rasing: Phys. Rev. Lett. **78**, 2004 (1997)
23. V.V. Pavlov, R.V. Pisarev, A. Kirilyuk, Th. Rasing: J. Appl. Phys. **81**, 4631 (1997)
24. R. Stolle, G. Marowsky, E. Schwarzberg, G. Berkovic: Appl. Phys. B **63**, 491 (1996)
25. O.A. Aktsipetrov, P.V. Elyutin, A.A. Nikulin, E.A. Ostrovskaya: Phys. Rev. B **51**, 17 591 (1995)